MethodsX 8 (2021) 101414

Contents lists available at ScienceDirect

MethodsX

journal homepage: www.elsevier.com/locate/mex

Method Article

A miniaturized optoelectronic biosensor for real-time point-of-care total protein analysis

Ophir Vermesh[a,b,1,*], Fariah Mahzabeen[c,1], Jelena Levi[a,b], Marilyn Tan[d], Israt S. Alam[a,b], Carmel T. Chan[a,b], Sanjiv S. Gambhir[a,b,e,f,2], James S. Harris[c,*]

[a] Department of Radiology, Stanford University, Stanford, CA, 94305, USA
[b] Molecular Imaging Program at Stanford, Stanford University, Stanford, CA 94305, USA
[c] Department of Electrical Engineering, Stanford University, Stanford, CA, 94305, USA
[d] Department of Medicine, Stanford University, Stanford, CA 94305, USA
[e] Department of Bioengineering, Stanford University, Stanford, CA 94305, USA
[f] Stanford Bio-X, Stanford University, Stanford, CA 94305, USA

A B S T R A C T

A miniaturized optoelectronic sensor is demonstrated that measures total protein concentration in serum and urine with sensitivity and accuracy comparable to gold-standard methods. The sensor is comprised of a vertical cavity surface emitting laser (VCSEL), photodetector and other custom optical components and electronics that can be hybrid packaged into a portable, handheld form factor. In conjunction, a custom fluorescence assay has been developed based on the protein-induced fluorescence enhancement (PIFE) phenomenon, enabling real-time sensor response to changes in protein concentration. Methods are described for the following:

- Standard curves: Used to determine the sensitivity, dynamic range, and linearity of the VCSEL biosensor/PIFE assay system in buffer as well as in human blood and urine samples.
- Comparison of VCSEL biosensor performance with a benchtop fluorimetric microplate reader.
- Accuracy of the VCSEL biosensor/PIFE assay system: Evaluated by comparing sensor measurements with gold-standard clinical laboratory measurements of total protein in serum and urine samples from patients with diabetes.

DOI of original article: 10.1016/j.bios.2020.112823
* Corresponding authors.
E-mail addresses: overmesh@stanford.edu (O. Vermesh), jharris@stanford.edu (J.S. Harris).
[1] These authors contributed equally to this paper.
[2] This paper is dedicated to the memory of Prof. Sanjiv Sam Gambhir.

https://doi.org/10.1016/j.mex.2021.101414

ARTICLE INFO
Method name: VCSEL Biosensor Design and PIFE-Based Total Protein Analysis
Keywords: Sensor, VCSEL, PIFE, Diabetes, Nephropathy, Urine, Total protein
Article history: Received 15 March 2021; Accepted 14 June 2021; Available online 17 June 2021

Specifications table

Subject area:	Medicine and dentistry
More specific subject area:	*Biosensors*
Method name:	VCSEL Biosensor Design and PIFE-Based Total Protein Analysis
Name and reference of original method:	Mahzabeen F., et al., Real-time point-of-care total protein measurement with a miniaturized optoelectronic biosensor and fast fluorescence-based assay, Biosens. Bioelectron. (2020) 112823.
Resource availability:	*N/A*

Method details

Objective

The objective of this study was to design a miniaturized fluorescence-based sensor capable of rapid, reliable, and sensitive detection of total protein levels in patient serum and urine samples with applications in point-of-care and at-home monitoring of diabetic kidney disease. A vertical-cavity surface-emitting laser (VCSEL) was hybrid integrated with a PIN photodetector and optical filters in a single device. Instantaneous detection of protein in serum or urine samples was enabled via protein-induced fluorescence enhancement (PIFE) of a near-infrared cyanine dye (Fig. 1). Proteins interact non-covalently with cyanine dyes, increasing fluorescence quantum yield and excited-state lifetime by stabilizing the dyes' photoactive *trans* conformation in the excited state [1,2]. Previous biosensor designs employing VCSELs for sample analysis involved the use of antibodies, multiple incubation and wash steps, [3] and external optical components, [3–5] rendering them expensive, time-consuming, and nonportable. Our biosensor integrates all optical components within a small device footprint and employs an antibody-free single-step assay. Discrete integration also overcomes performance limitations seen with monolithic integration of the optical components on a single substrate, including interlayer and lateral optical crosstalk between the laser and photodector. [6,7] This work is the first demonstration to our knowledge of a VCSEL sensor coupled with a PIFE assay for real-time sample analysis of total protein concentrations.

Sensor design

The VCSEL biosensor operates in the near infrared region. Two commercially available 675 nm VCSELs (Vixar, Plymouth, MN) and a custom-fabricated PIN GaAs detector are wire bonded on a TO-5 (Transistor Outline, Case Style 5) metal can package (Package number H10C, Texas Instruments, Dallas, TX). The advantages of using PIN photodetectors include lower power consumption, small size, and simple, low cost integration [8]. Optical cross-talk is minimized by spatially separating the VCSEL from the detector with a quartz spacer and by use of a Ti/Au baffle (Fig. 2a). Background interference is minimized by placing the VCSEL and detector in a coplanar arrangement, painting the package sidewalls black to reduce stray light reflection, and situating filters on top of the detector that pass 750 $\pm$ 20 nm fluorescence emission and reject six order of magnitude of 675 nm excitation light. Filters include an integrated dielectric notch filter (Chroma Technology, Bellows Falls, VT) and a hybrid bonded fluorescence emission filter incorporating a 2 mm thick layer of RG695 absorbing glass (Chroma Technology, Bellows Falls, VT). The VCSEL's narrow laser line width also minimizes scattered excitation interference. The 9 mm sensor package (Fig. 2a) is mounted with an anti-reflective

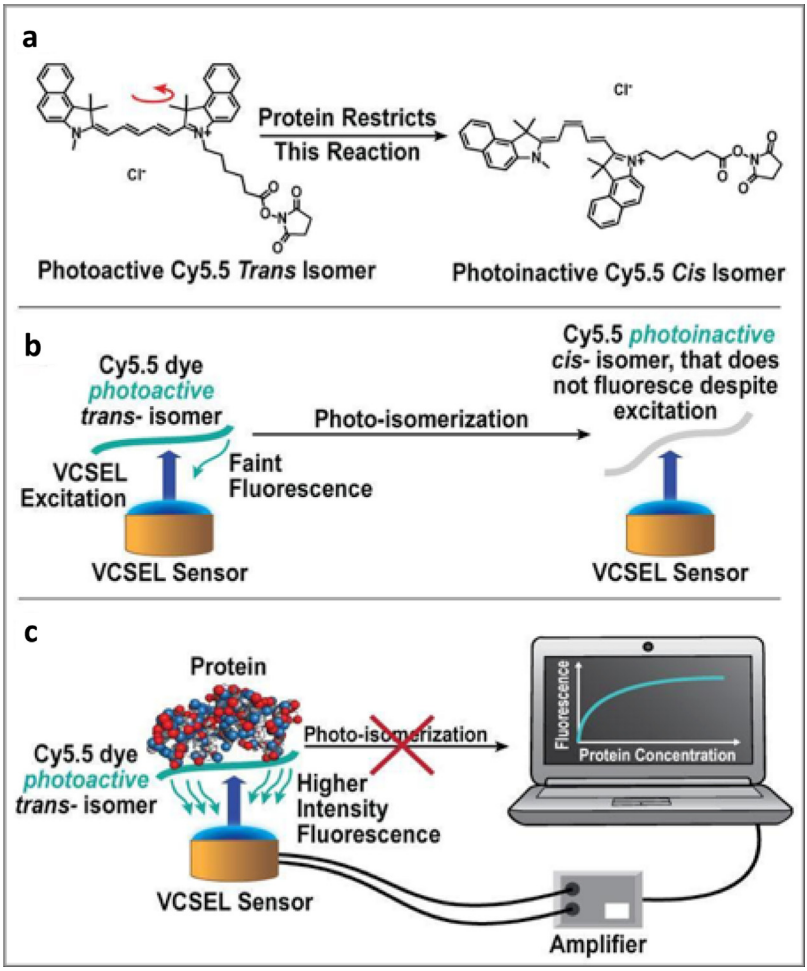

Fig. 1. *Protein-induced fluorescence enhancement of a cyanine dye.* (**a**) Cyanine dyes photo-isomerize between a photoactive *trans* isomer and a photoinactive *cis* isomer. (**b**) The photoactive *trans* isomer fluoresces upon excitation and undergoes photoisomerization, converting to the fluorescently inactive *cis* isomer. **c.** When a protein non-covalently interacts with the dye, it stabilizes the *trans* conformation in the photoactive state, resulting in a longer excited-state lifetime and higher quantum yield. The VCSEL laser excites the sample and a hybrid-integrated photodetector captures the emitted fluorescence, producing a current in proportion to protein concentration.

collimation lens (NA=0.55, Thorlabs, Newton, NJ) and placed in a cage (~1.5 inches) that holds a sample well (AK05-0105, Avioq, Durham,NC) ~1 mm above the sensor (Fig. 2b). The cage is built with black metal optical mounts (Thorlabs, Newton, NJ) and provides further shielding from external light interference. External electronics include a computer, signal generator (Keithley 6221, Keithley Instruments, Cleveland, OH), and lock-in amplifier (SR830, Stanford Research Systems, Sunnyvale, CA) (Fig. 2c). After designing and assembling the VCSEL biosensor, we characterized its signal response, linearity, sensitivity, and dynamic range in buffer as well as in human blood and urine. We then compared the sensor's performance to that of a benchtop fluorimeter. Finally, we tested the accuracy of our sensor on clinical urine samples from patient with diabetes by comparing sensor measurements with values obtained using a gold standard method.

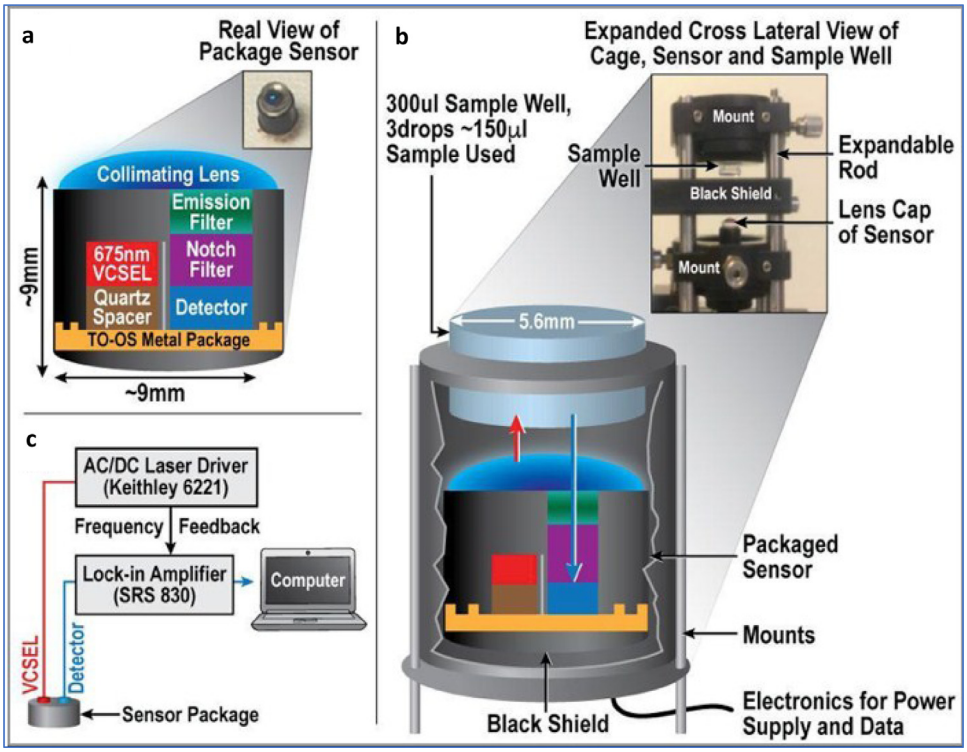

Fig. 2. *Schematic of VCSEL sensor design.* (**a**) Cross-sectional view of the biosensor showing the optical components - VCSEL, PIN photodetector, and optical filters - incorporated within a ~9 mm TO-5 metal package with a collimation lens. The package sidewalls are painted black to reduce stray light reflection. The coplanar arrangement of the VCSEL and detector minimizes background interference. A quartz spacer is used to separate the VCSEL from the detector, further minimizing optical cross-talk. The combination of an emission filter and dielectric notch filter on top of the photodetector passes fluorescence emission centered at 750 nm with a bandwidth of 40 nm and rejects six order of magnitude of 675 nm excitation light. (**b**) Sample analysis setup with a 300 µL sample well situated directly above the VCSEL sensor from (a). The sample well contains 150 µL total volume of a diluted biofluid sample (serum or urine) mixed with 1 µL of Cy5.5 dye (1 mg/mL Cy5.5). Inset image: Exploded view of the setup. (**c**) Block diagram of the sensor connected to a lock-in amplifier, external laser driver, switch, and computer. These electronic components are commercially available in miniaturized form, which could allow for complete integration with the sensor in a portable handheld device with a 7-inch form factor.

Sensor operation

With the sensor switched on, a biofluid sample is first diluted in buffer to a total volume of ~150 µL within the 300 µL sample well. Urine samples are diluted 10-fold whereas serum samples are diluted 100-fold. One microliter of a 1 mg/mL Cy5.5 dye solution in dimethylformamide (DMF) (Sigma-Aldrich, St. Louis, MO) is then added and mixed. Alternatively, the sample solution can be premixed with dye and then transferred to the sample well. As the VCSEL laser excites the sample, the photodetector captures the fluorescence emission. Excitation VCSELs have the following parameters: 0.75 – 1.0 mW average optical output power at 675 nm (at room temperature); current-driven with a sinusoidal 23 Hz waveform (2 mA peak-to-peak); 1.5 mA threshold current; ~0.40 slope efficiency, 8 mA DC offset. The GaAs detectors exhibit quantum efficiencies over 75% and dark currents less than 5 pA/mm [2] for 100 mV bias. The detector output signal is amplified and filtered in real-time by a lock-in amplifier (time constant: 30 ms; sensitivity: 20 mV). The instruments are controlled over a GPIB interface by a MatLab (Mathworks, Natick, MA) program.

Standard solutions

The albumin-to-immunoglobulin ratio in serum is approximately 10:7. We created a protein cocktail in buffer that simulated this protein composition by combining 0.1% human serum albumin (HSA) (Sigma-Aldrich, St. Louis, MO) and 0.1% immunoglobulin G (IgG) (Sigma-Aldrich, St. Louis, MO) solutions in a 10:7 ratio in phosphate-buffered saline (PBS) (Gibco, Thermo Fisher Scientific, Waltham, MA). For standard solutions of protein-spiked buffer, two-fold serial additions of this protein solution (starting with 4 µL) in PBS (to 149 µL total volume) were carried out in separate microcentrifuge tubes. We then created serum-containing standard solutions with a wide range of protein concentrations (0.03 – 4.1 g/L) by serially spiking pooled human serum (Stanford Blood Bank, Stanford, CA) in two-fold increments (starting at 0.5 μL) into PBS (to 149 μL total volume) in separate microcentrifuge tubes. Finally, we created urine standard solutions with protein concentrations spanning from 0.013 g/L to 8.6 g/L. After testing a number of different dilutions of urine samples in PBS, we found that a 10-fold dilution was optimal in maintaining good sensitivity for protein analysis while minimizing background interference from the urine matrix. To create the standard solutions, we spiked a 0.1% HSA/PBS solution in increasing quantities into normoalbuminuric urine (Stanford Diabetes Clinic, Stanford, CA) and diluted 10-fold in PBS (up to 149 µL total volume). For all standard solutions, one microliter of Cy5.5 dye solution was added to each tube (150 µL final volume), the tubes were vortexed for 3 s to ensure uniform mixing, and the samples were tested with the VCSEL biosensor to obtain a standard curve.

Clinical urine samples

All urine samples obtained from patients at the Stanford Diabetes Clinic were collected and processed in accordance with and permission from the Stanford Institutional Review Board. An initial set of urine samples ($n = 5$) were collected in plastic urine collection cups, which were immediately sealed and stored on ice and were subsequently either stored frozen at −20 °C for future testing or tested within 1–2 h. Additional urine samples, pre-tested by urine dipstick, from diabetic patients ($n = 9$) were purchased from an outside vendor (Lee Biosolutions, Maryland Heights, MO). We performed urine dipstick testing (or re-testing) of all urine samples, and protein content was assessed semi-quantitatively (normal, trace, 1+, 2+, 3+, 4+) against color codes on the package label. We then tested urine samples (diluted 10-fold in PBS) quantitatively for total protein using the VCSEL biosensor and benchtop fluorimetric instruments.

Fluorescence measurements

Diluted serum or urine samples as well as calibration standards (149 uL sample/standard + 1 μL Cy5.5 dye) were pipetted into a 96-well black microtiter plate in triplicate. For fluorescence readout, a Synergy 4 benchtop microplate reader (BioTek, Winooski, VT) was used in fluorescence mode with 675 nm excitation and 710 nm emission. Readings were acquired at room temperature with a 1-second acquisition time per sample. The microtiter plate was then separately tested within an IVIS Spectrum in vivo imaging system (Perkin Elmer, Waltham, MA) and fluorescence images were acquired with the following settings: 675 nm filter; 2 second exposure time; medium binning; f-stop of 2. To measure the average radiance, a region of interest was drawn around each sample well in the acquired image, and the control (buffer and dye only) signal was subtracted.

Sensor accuracy

To assess the accuracy of the sensor in measuring protein concentrations in serum, VCSEL biosensor measurements of serum-spiked buffer samples were compared with gold standard values of the same solutions obtained using the Pierce Bicinchoninic acid (BCA) Protein Assay Kit (Thermo Fisher Scientific, Waltham, MA) according to the manufacturer's protocol. To assess the accuracy of the sensor in measuring protein concentrations in urine samples, VCSEL biosensor measurements of diluted urine samples were compared with values obtained by microalbumin testing at the Stanford

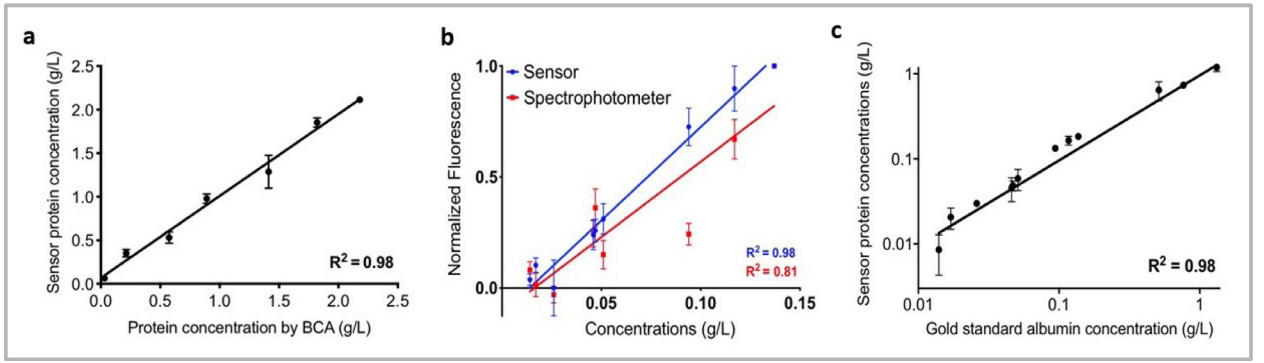

Fig. 3. *Accuracy of the VCSEL biosensor and performance comparison with benchtop fluorimetry.* **(a)** Protein concentrations of various serum dilutions were interpolated from a standard curve of protein-spiked buffer (not shown) based on their sensor signal. The sensor-derived serum protein concentrations were plotted above against the actual protein concentrations of the samples as determined by BCA analysis ($y = 0.94x + 0.07$). **(b)** Linear range of urine protein concentrations measured by the sensor ($y = 8.41x - 0.12$) and benchtop fluorimeter ($y = 6.79x - 0.11$). Due to the use of different units in the two methods, fluorescence signals at each concentration were normalized to the maximum linear (pre-saturation) signal. The two methods are strongly correlated (Pearson $R = 0.82$, p-value < 0.001). **(c)** To evaluate sensor accuracy and the suitability of urine total protein as a surrogate marker for urine albumin concentration, sensor total protein measurements were plotted against gold standard micoalbumin for urine protein concentrations in the range of 0 – 1.0 g/L (Pearson $R = 0.99$, p-value < 0.0001). Best-fit line: $y = 0.96x$ ($R^2 = 0.98$). Data points represent the mean ± s.d. of $n = 3$ independent samples. Note: Some error bars are too small to be visible on the scale of the graphs.

Clinical Laboratory using gold standard immunonephelometry on a Dimension Vista (Siemens AG, Munich, Germany) chemistry analyzer.

Data analysis

All data presented in this paper represent the mean ± standard deviation (SD) of triplicate samples. Sample and standard solution fluorescence signals were background subtracted by blank control samples (buffer + dye) to obtain net fluorescence signals. A 5-parameter logistic function (generalized Hill equation) was used as a best-fit curve of the standard solution fluorescence intensities [9]. The linear portions of the curves were separately analyzed by linear regression. Goodness of fit was assessed using R^2 correlation coefficients. Protein concentrations in serum and urine were interpolated from the best-fit curves. The limits of detection (LOD) and quantification (LOQ) were calculated using: $LOD = \frac{3 \times SD}{s}$ and $LOQ = \frac{10 \times SD}{s}$, where s is the slope of the response curve and SD is the standard deviation of the residuals (from the regression line). [10] Coefficients of variation (CV) were calculated using: $CV = (SD/Mean) \times 100$. To assess accuracy, sensor and gold standard measurements were correlated using a Pearson R-value and two-tailed P-value. GraphPad Prism 5 (Graphpad Software Inc., San Diego, CA) was used for statistical and graphical analysis.

Method validation

A calibration curve was generated from standard solutions of protein-spiked buffer and the concentrations of diluted serum samples were interpolated from this curve based on their sensor signals. The sensor-derived concentrations were compared against the actual sample protein concentrations as determined by BCA protein analysis and yielded an accuracy curve with a slope close to unity (0.94) and y-intercept close to zero ($R^2 = 0.98$) (Fig. 3a). The average intra-assay CV was 5.7%. We then compared the performance of the sensor with that of a benchtop microplate reader by running standard solutions of protein-spiked urine on both devices. Since the output from the sensor is in units of amperes while the output from the microplate reader is in arbitrary fluorescence intensity units, we normalized both sets of measurements and plotted them for comparison. Sensor and fluorimeter best-fit curves correlated well with each other (Pearson $R = 0.82$, p-value <0.001) (Fig. 3b).

Proteinuria is a strong predictor of unfavorable outcomes in chronic kidney disease. Measurement of urine total protein is more amenable to antibody-free analysis than measurement of urine albumin. However, urine albumin is the more commonly used biomarker for detecting early kidney disease in diabetes. [11,12] Therefore, we next evaluated whether our sensor's urine total protein measurements could serve as a reliable surrogate for urine albumin in patients with diabetes. We tested each clinical urine sample ($n = 14$) with the sensor and plotted the sensor total protein measurements against urine microalbumin (the gold standard immunonephelometric test for urine albumin) (Figs. 3c). Urine total protein correlated strongly with microalbumin across a wide range of clinical urine albumin levels (Pearson $R = 0.92$, p-value < 0.0001). The correlation between sensor and gold standard measurements was particularly high for urine protein concentrations in the range of 0.02 – 1.0 g/L (p-value < 0.0001, Pearson $R = 0.99$). The LOD and LOQ for urine total protein were 0.023 g/L and 0.075 g/L, respectively. [13]

Declaration of Competing Interest

The Authors confirm that there are no conflicts of interest.

Acknowledgments

We would like to acknowledge the Canary Center at Stanford for Cancer Early Detection, the Stanford Health Care clinical laboratories for performing microalbumin testing on clinical urine samples, and James Strommer for figure design. Funding: This research was supported by a grant from the Canary Foundation. Author contributions: OV, FM, JL, SSG, and JH conceived of the project

idea. FM designed the sensor customized for in-vitro sampling of small liquid volumes. OV conceived of using a PIFE-based assay for total protein analysis and guided its validation on clinical samples. FM and OV performed the experiments. OV and FM analyzed the data and wrote the manuscript. JL advised on the chemistry aspects of the experiments. MT provided guidance and patient samples for the clinical study. ISA helped with IVIS experiments and BCA protein measurements. CTC edited the manuscript and provided insightful suggestions and comments. JH, SSG, and OV supervised the project. All authors discussed the results and contributed to the final manuscript.

Supplementary materials

Supplementary material associated with this article can be found in the online version at doi:10.1016/j.mex.2021.101414.

References

[1] E.M. Stennett, M.A. Ciuba, S. Lin, M. Levitus, Demystifying PIFE: the photophysics behind the protein-induced fluorescence enhancement phenomenon in Cy3, J. Phys. Chem. Lett. 6 (2015) 1819–1823.
[2] E.M. Stennett, M.A. Ciuba, M. Levitus, Photophysical processes in single molecule organic fluorescent probes, Chem. Soc. Rev. 43 (2014) 1057–1075.
[3] C.F. Mateus, et al., Digest of the LEOS summer topical meetings biophotonics, in: Proceedings of the Optical Interconnects and VLSI Photonics/WBM Microcavities, 2004, IEEE, 2004, p. 2.
[4] C.F. Mateus, M.C. Huang, P. Li, B.T. Cunningham, C.J. Chang-Hasnain, Compact label-free biosensor using VCSEL-based measurement system, IEEE Photon. Technol. Lett. 16 (2004) 1712–1714.
[5] K. Nakazato, Chemistry integrated circuit: chemical system on a complementary metal oxide semiconductor integrated circuit, Philos. Trans. R. Soc., A 372 (2014) 20130109.
[6] T. O'Sullivan, et al., Implantable semiconductor biosensor for continuous in vivo sensing of far-red fluorescent molecules, Opt Express 18 (2010) 12513–12525.
[7] T.D. O'Sullivan, Implantable fluorescence sensor for continuous molecular monitoring in live animals, Dissertation for Doctor of Philosophy, Stanford University, 2010.
[8] M. Cvijetic, Optical Transmission Systems Engineering, Artech House, 2004.
[9] J. Giraldo, N.M. Vivas, E. Vila, A. Badia, Assessing the symmetry of concentration-effect curves: empirical versus mechanistic models, Pharmacol. Ther. 95 (2002) 21–45.
[10] A. Shrivastava, V.B. Gupta, Methods for the determination of limit of detection and limit of quantitation of the analytical methods, Chron. Young Sci. 2 (2011) 21.
[11] E.J. Lamb, F. MacKenzie, P.E. Stevens, How should proteinuria be detected and measured? Ann. Clin. Biochem. 46 (2009) 205–217.
[12] H. Martin, Laboratory measurement of urine albumin and urine total protein in screening for proteinuria in chronic kidney disease, Clin. Biochem. Rev. 32 (2011) 97.
[13] F. Mahzabeen, et al., Real-time point-of-care total protein measurement with a miniaturized optoelectronic biosensor and fast fluorescence-based assay, Biosens. Bioelectron. (2020) 112823.